Optical Fiber Design for Field Mountable Connectors

Ming-Jun Li and Costas Saravanos

***Abstract*—This paper presents a study on optical fiber and connector ferrule assembly design optimization aimed at minimizing modal interference in field-mountable single-mode fiber connectors that utilize a ferrule mounted short fiber stubs and integrated splices. A theoretical model for analyzing the modal interference is proposed and verified experimentally. It is shown that modal interference can be reduced by optimizing both the fiber design and its surrounding material.**

***Index Terms*—Connector ferrule assembly, coupling efficiency, cutoff wavelength, depressed cladding fiber, fiber connector, fiber splice, fiber stub, field-mountable connector, fundamental mode, higher order modes, insertion loss, leaky loss, matched cladding fiber, modal interference, scalar wave equation, single-mode fiber (SMF).**

I. Introduction

THERE has been an increasing interest in a new generation of field-mountable connectors. In these connectors, a 5- to 15-mm piece of optical fiber is epoxied in a straight-tip ferrule. One end of the ferrule is factory polished, while the other is integrated into a mechanical or fusion splice [1]. This whole assembly, called the stub, is linked to the fiber in the field through the same mechanical splice.

This type of optical fiber connector has the advantage of eliminating the use of epoxies and polishing in the field. At the same time, the connector quality is guaranteed since the most crucial part of its assembly is completed in the factory. However, a mated pair of this connector design introduces three closely spaced discontinuities (two splices and a connection point between them) that may result in modal interference [2]–[7].

Generally speaking, single-mode fibers (SMF's) used in telecommunications applications in the 1310-nm operating window, are not purely single mode. There exists higher order modes that propagate in the whole fiber structure consisting of fiber core, claddings and surrounding materials. These higher order modes have high attenuation coefficients that depend on the fiber length, the operating wavelength and the layout condition. For standard single-mode fibers of a few meters in length, these modes are completely attenuated at 1310 nm and not observed. At lengths significantly shorter than one meter or at short operating wavelengths, they may carry significant power.

The phenomenon of modal interference is observed when a short piece of fiber (B) is connected between two other fibers (A) and (C), as shown in Fig. 1. Light from the fundamental LP_{01} mode of the launching fiber (A) that is lost in the first splice is coupled into the higher order modes of the fiber (B). In the second splice, some of the light in the higher order modes is coupled from (B) back to the LP_{01} mode of the receiving fiber (C) and interferes with the light already resident there. This interference causes fluctuations of the transmitted power as a function of wavelength. As the laser-operating wavelength varies, the connector loss can change due to the modal interference, significantly increasing the chance of the failure of a telecommunication system. Furthermore, because the modal interference depends on the stub length and operating wavelength, the connector loss is unpredictable. The development of this type of connector can succeed only if the modal interference is reduced significantly.

The objective of this work is to design and fabricate a special fiber type and ferrule assembly, where the modal interference effects are minimized without connection loss increase. In this work, the modal interference is studied theoretically and experimentally. By optimizing both the fiber design and the properties of the material that surrounds the fiber (i.e., the connector ferrule assembly), the modal interference is reduced.

Manuscript received March 24, 1999.

M.-J. Li is with the Telecommunications Product Division, Corning, Inc., Corning, NY 14831 USA (e-mail: lim@corning.com).

C. Saravanos is with Siecor, Keller, TX 76248 USA (e-mail: costas_saravanos@siecor.com).

Publisher Item Identifier S 0733-8724(00)02295-7.

II. Theoretical Approach

A. Transmission Efficiency in One- and Two-Stub Systems

Previously, a theoretical model had been developed for calculating the transmission efficiency of a system containing one or two short pieces of fiber [8], [9]. This model assumes that power conversion in each splice occurs between the LP_{01} and LP_{11} modes only and is valid for fibers of a few meters long at operating wavelengths below the cutoff wavelength. In this case the LP_{11} mode dominates the other higher order modes. It has been found that, for fibers of a few centimeters long (stubs), the modal interference exists even for wavelengths above the cutoff wavelength. This indicates that for a fiber stub, the higher order modes carry significant power and are the main contributors to modal interference. We develop here a more general model by taking into account the existence of other higher order modes.

For a one-stub system (Fig. 1), suppose that the coupling coefficient of the LP_{01} mode from the launching fiber to the stub is $\eta^{(1)}_{01\,01}$ in the first joint, and from the stub to the receiving fiber is $\eta^{(2)}_{01\,01}$ in the second joint. The coupling coefficient from the LP_{01} mode to a higher order mode LP_{lm} is $\eta^{(1)}_{01\,lm}$ in the first joint, and the coupling coefficient from the LP_{lm} to the LP_{01} mode is $\eta^{(2)}_{lm\,01}$ in the second joint. The transmission efficiency of the LP_{01} mode is expressed as

$$\eta = \eta^{(1)}_{01\,01}\eta^{(2)}_{01\,01} + \sum_{l,m} \eta^{(1)}_{01\,lm}\eta^{(2)}_{lm\,01} \exp(-2\alpha_{lm}L)$$

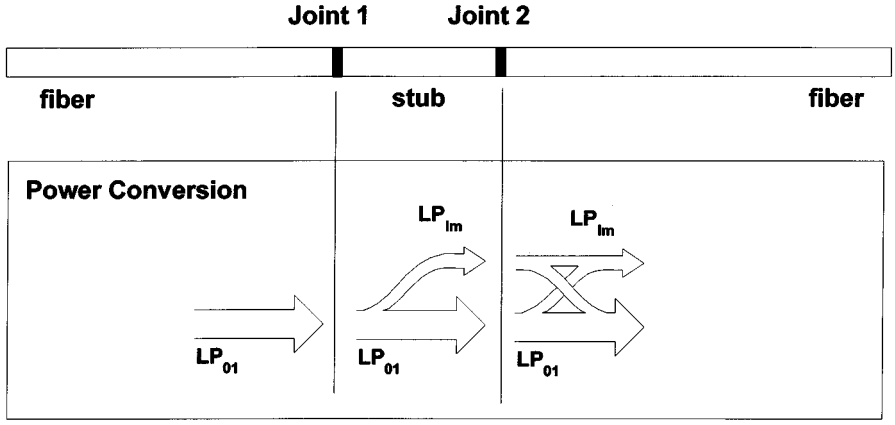

Fig. 1. Modal interference schematic for one-stub case.

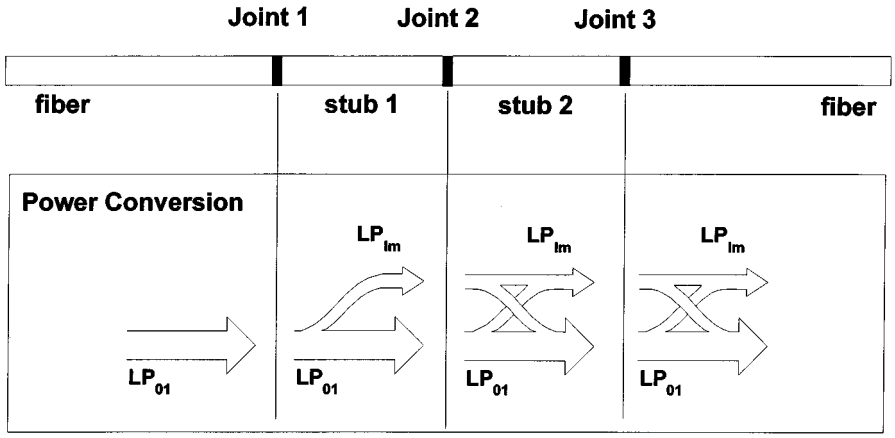

Fig. 2. Modal interference schematic for two-stub case.

$$+\sum_{l,m} 2\sqrt{\eta^{(1)}_{01\,01}h^{(2)}_{01\,01}h^{(1)}_{01\,lm}h^{(2)}_{lm\,01}} \cdot \exp(-\alpha_{lm}L)\,\cos(\Delta\beta_{lm}L) \tag{1}$$

where

L is the length of the fiber stub;

α_{lm} is the attenuation coefficient of the LP_{lm} mode;

$\Delta\beta_{lm}$ is the difference in propagation constant between the LP_{lm} and the LP_{01} modes.

In the above expression, we have neglected the cross terms between two higher order modes, since they contribute much less than the cross terms between the LP_{01} and the higher modes.

For a two-stub system (Fig. 2), we use a similar notation and neglect the cross terms between two higher order modes

$$\begin{aligned}\eta =& \eta^{(1)}_{01\,01}\eta^{(2)}_{01\,01}\eta^{(3)}_{01\,01} \\ &+\sum_{l,m}\eta^{(1)}_{01\,lm}\eta^{(2)}_{lm\,01}\eta^{(3)}_{01\,01}\exp(-2\alpha_{lm}L_1) \\ &+\sum_{l,m}\eta^{(1)}_{01\,01}\eta^{(2)}_{01\,lm}\eta^{(3)}_{lm\,01}\exp(-2\alpha_{lm}L_2) \\ &+\sum_{l,m}\eta^{(1)}_{01\,lm}\eta^{(2)}_{lm\,lm}\eta^{(3)}_{lm\,01}\exp[-2\alpha_{lm}(L_1+L_2)] \\ &+\sum_{l,m}2\sqrt{\eta^{(1)}_{01\,lm}\eta^{(2)}_{lm\,01}\eta^{(3)}_{01\,01}\eta^{(1)}_{01\,01}\eta^{(2)}_{01\,lm}\eta^{(3)}_{lm\,01}} \\ &\cdot\exp[-2\alpha_{lm}(L_1+L_2)]\cos[\Delta\beta_{lm}(L_1-L_2)] \\ &+\sum_{l,m}2\left[\sqrt{\eta^{(1)}_{01\,01}\eta^{(2)}_{01\,01}\eta^{(3)}_{01\,01}\eta^{(1)}_{01\,lm}\eta^{(2)}_{lm\,01}\eta^{(3)}_{01\,01}}\right. \\ &\left.+\sqrt{\eta^{(1)}_{01\,01}\eta^{(2)}_{01\,lm}\eta^{(3)}_{lm\,01}\eta^{(1)}_{01\,lm}\eta^{(2)}_{lm\,lm}\eta^{(3)}_{lm\,01}}\exp(-2\alpha_{lm}L_2)\right] \\ &\cdot\exp(-\alpha_{lm}L_1)\cos(\Delta\beta_{lm}L_1) \\ &+\sum_{l,m}2\left[\sqrt{\eta^{(1)}_{01\,01}\eta^{(2)}_{01\,01}\eta^{(3)}_{01\,01}\eta^{(1)}_{01\,01}\eta^{(2)}_{01\,lm}\eta^{(3)}_{lm\,01}}\right. \\ &\left.+\sqrt{\eta^{(1)}_{01\,lm}\eta^{(2)}_{lm\,01}\eta^{(3)}_{01\,01}\eta^{(1)}_{01\,lm}\eta^{(2)}_{lm\,lm}\eta^{(3)}_{lm\,01}}\exp(-2\alpha_{lm}L_1)\right] \\ &\cdot\exp(-\alpha_{lm}L_2)\cos(\Delta\beta_{lm}L_2) \\ &+\sum_{l,m}2\sqrt{\eta^{(1)}_{01\,01}\eta^{(2)}_{01\,01}\eta^{(3)}_{01\,01}\eta^{(1)}_{01\,lm}\eta^{(2)}_{lm\,lm}\eta^{(3)}_{lm\,01}} \\ &\cdot\exp[-2\alpha_{lm}(L_1+L_2)]\cos[-\Delta\beta_{lm}(L_1+L_2)]\end{aligned} \tag{2}$$

where L_1 and L_2 are the length of the first and second fiber stub, respectively. The transmission efficiency of the two-stub system, which contains more terms than the one-stub system, seems very complicated. But if we take a look at the terms that contribute to modal interference, the two-stub system is easily understood in terms of the one-stub case. There are four oscillation terms in (2), each one corresponding to an oscillation of a single stub with lengths of $|L_1-L_2|$, L_1, L_2, and L_1+L_2. The

contribution of the term containing $(L_1 - L_2)$ is negligible, since optimized connectors have an equal fiber length. The problem thus reduces to the superposition of oscillations of three stubs. In the following analysis we consider only the single-stub case.

Equation (1) shows that modal interference periods are governed by the fiber length and the difference in propagation constant between the fundamental and the higher order modes. The power variation amplitude depends on the splice loss, the attenuation coefficient of these higher order modes and their respective coupling efficiency to the fundamental mode. Therefore, in order to minimize the modal interference, an accurate knowledge of the mode properties, such as the effective refractive index, the attenuation coefficient, the power distribution of the fundamental and higher order modes, and the coupling efficiencies between the fundamental and the higher order modes is necessary.

B. Mode Properties

Fig. 3 represents a simplified waveguide structure of a fiber inserted into a connector ferrule. This guiding structure consists of four layers: the fiber core, the inner and outer claddings, and the surrounding material (connector ferrule). The refractive index of the ferrule material commonly used for connectors is higher than that of the outer cladding. Such a system supports a set of modes with complex propagation constants (leaky modes). These constants are calculated from the eigenvalue solution of the scalar wave equation

$$\frac{\partial^2\Psi}{\partial r^2} + \frac{1}{r}\frac{\partial\Psi}{\partial r} + \frac{1}{r^2}\frac{\partial^2\Psi}{\partial\theta^2} + (k_0^2 n^2 - \gamma^2)\Psi = 0. \tag{3}$$

For a step-index profile, the solution of this equation is a combination of Bessel and Hankel functions:

$$(r,\,\theta) = \left\{ \begin{array}{c} A_1 J_l(u_1 r) \\ A_2 H_l^{(1)}(u_2 r) + B_2 H_l^{(2)}(u_2 r) \\ A_3 H_l^{(1)}(u_3 r) + B_3 H_l^{(2)}(u_3 r) \\ A_4 H_l^{(1)}(u_4 r) \end{array} \right\} \cdot [\sin(l\theta),\ \cos(l\theta)] \tag{4}$$

where

$$u_i = \sqrt{k_0^2 n_i^2 - \gamma^2}$$

$(i = 1, 2, 3, 4)$, J_l is the Bessel function of the first kind, and $H_l^{(1)}$ and $H_l^{(2)}$ are the Hankel functions of the first kind and the second kind. The continuities of the fields and their derivatives at the interfaces lead to the eigenvalue equation shown in (5) at the top of the next page. By looking for solutions in the complex plane, the complex propagation constant of the leaky modes can be found. From the real and imaginary parts of the propagation constant, we obtain the effective index and the leaky loss of these higher order modes. Their field distribution is calculated from the eigenfunction of the wave equation.

C. Coupling Efficiencies

The coupling efficiencies needed to evaluate the modal interference amplitude are calculated from (6) shown at the bottom of the next page [7], where A is the fiber cross-sectional area

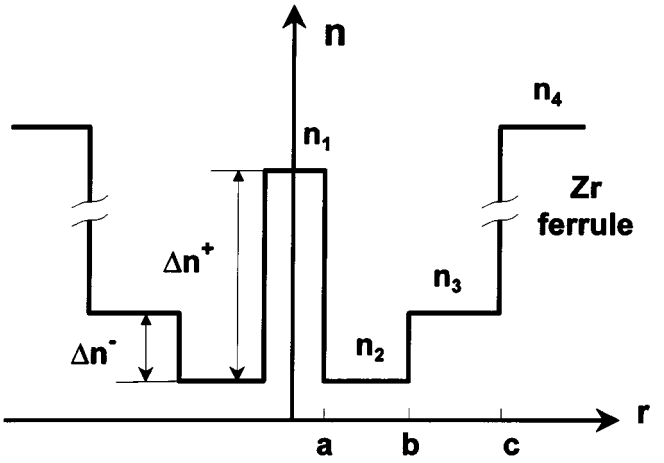

Fig. 3. Refractive index profile of optical waveguide.

(diameter of 125 μm) and A' the area of intersection of the two joined fibers. In this calculation, we have used the bounded mode approximation [10] for the leaky modes by taking the field intensity outside the fiber cross section to be equal to zero. The coupling efficiencies are calculated by assuming that the optical axes of the two fibers are offset with each other by a known distance. The longitudinal and angular offsets are neglected because, in a properly designed connector or mechanical splice, the contribution of these two components to the insertion loss is very small.

D. Modal Interference Amplitude

Once the effective indices, leaky losses, and coupling efficiencies of the fundamental and the higher order modes are known, the modal interference amplitude is evaluated using (1). The maximum total modal interference amplitude is calculated by adding the amplitude of all oscillation terms together, while assuming that they are all in phase.

III. Calculated Results and Discussion

Using the theory developed above, modal interference amplitudes for different fiber designs are calculated. In all the calculations shown below, the length of fiber stub is 15 mm. The cutoff wavelength of fibers is kept constant at 1089 nm. The core radius, a, and the refractive index difference, Δn, are chosen in such a way that the insertion loss due to the mode field diameter mismatch to a standard telecommunication fiber is minimized at 1310 and 1550 nm. The offset of the optical axes at the two splice points is assumed to be 1 μm, which corresponds to a total insertion loss of 0.35 dB. The surrounding material is zirconia with a refractive index of 2.2.

Fig. 4 shows the peak to peak oscillation amplitude at 1310 nm as a function of the index depression, Δn^-. The modal interference dependence at 1310 nm on the inner cladding to core diameter ratio, b/a, is plotted in Fig. 5. It is clear that high depression and small b/a reduce the modal interference. On the other hand, very small b/a increases the leaky loss of the fundamental mode, introducing additional connector loss. The increase in leaky loss of the fundamental mode as a function of b/a is plotted in Fig. 6. This figure shows that for b/a greater than

$$\begin{vmatrix} J_l(u_1r_1) & -H_l^{(1)}(u_2r_1) & -H_l^{(2)}(u_2r_1) & 0 & 0 & 0 \\ u_1J_l'(u_1r_1) & -u_2H_l^{(1)'}(u_2r_1) & -u_2H_l^{(2)'}(u_2r_1) & 0 & 0 & 0 \\ 0 & H_l^{(1)}(u_2r_2) & H_l^{(2)}(u_2r_2) & -H_l^{(1)}(u_3r_2) & H_l^{(2)}(u_3r_2) & 0 \\ 0 & u_2H_l^{(1)'}(u_2r_2) & u_2H_l^{(2)'}(u_2r_2) & -u_3H_l^{(1)'}(u_3r_2) & u_3H_l^{(2)'}(u_3r_2) & 0 \\ 0 & 0 & 0 & H_l^{(1)}(u_3r_3) & H_l^{(2)}(u_3r_3) & -H_l^{(1)}(u_3r_3) \\ 0 & 0 & 0 & u_3H_l^{(1)'}(u_3r_3) & u_3H_l^{(2)'}(u_3r_3) & u_4H_l^{(1)'}(u_4r_3) \end{vmatrix} = 0. \quad (5)$$

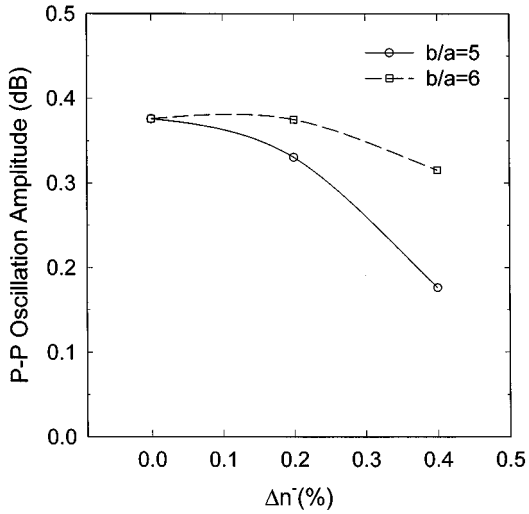

Fig. 4. P–P oscillation amplitude at 1310 nm as a function of Δn^- with insertion loss of 0.35 dB.

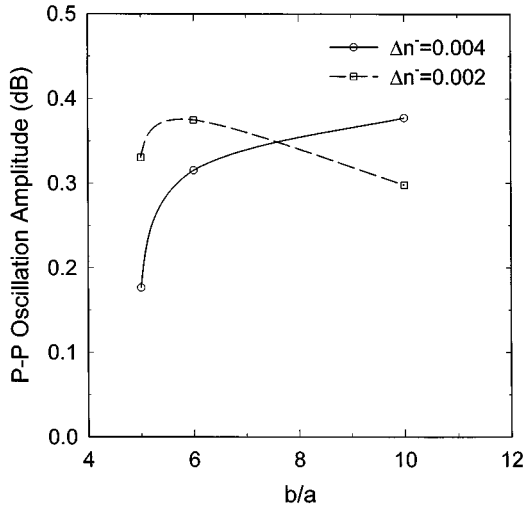

Fig. 5. P–P oscillation amplitude at 1310 nm as a function of b/a with insertion loss of 0.35 dB.

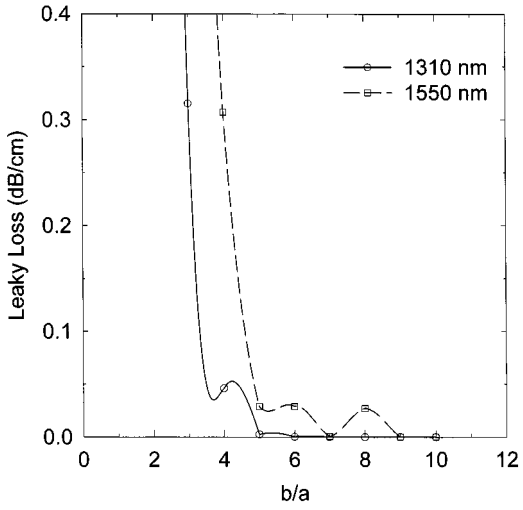

Fig. 6. Leaky loss of the fundamental mode as a function of b/a.

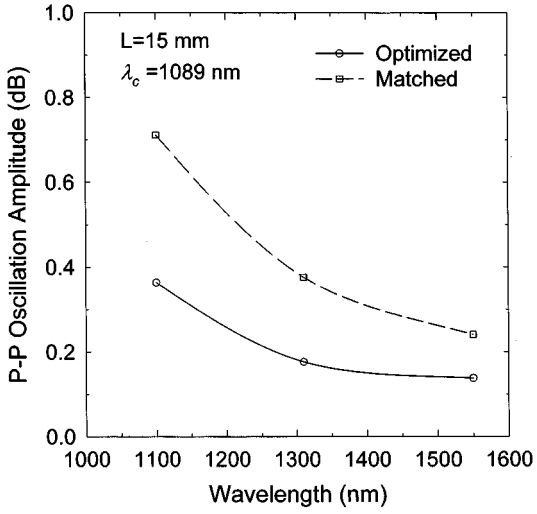

Fig. 7. P–P oscillation amplitude as a function of wavelength. The insertion losses at the wavelengths of 1100, 1310, and 1550 nm are 0.40, 0.35, and 0.30 dB, respectively.

five, the leaky loss of the fundamental mode is very small (less than 0.03 dB/cm) in the 1300–1550 nm wavelength window. For b/a smaller than five, the leaky loss increases drastically. From the above analysis, we conclude that an optimized fiber design must be fully depressed with b/a of 5.

Fig. 7 compares the calculated interference amplitude as a function of wavelength between an optimized and a matched cladding fiber design. This figure indicates that the modal interference in the optimized design is reduced significantly.

A further reduction in modal interference is achieved if the leaky loss of the higher order modes is increased by reducing the refractive index difference between the outer cladding and the surrounding ferrule material. Fig. 8 depicts the leaky loss as a function of the ferrule refractive index for the first leaky mode of both the optimized and matched cladding fiber designs. It is shown that for the matched cladding fiber, the refractive index of the ferrule must be matched exactly with the refractive index of the cladding in order to create sufficiently high leaky loss of the

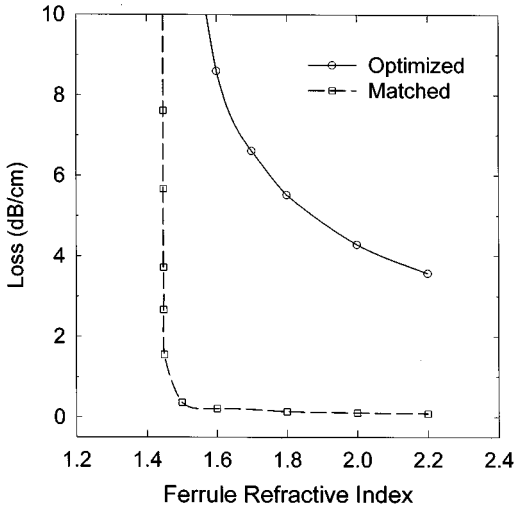

Fig. 8. Leaky loss of the first higher order mode as a function of ferrule refractive index.

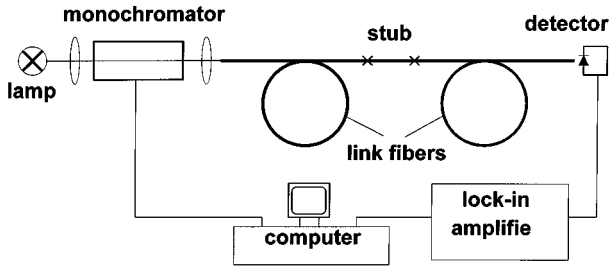

Fig. 9. Experimental setup for measuring modal interference.

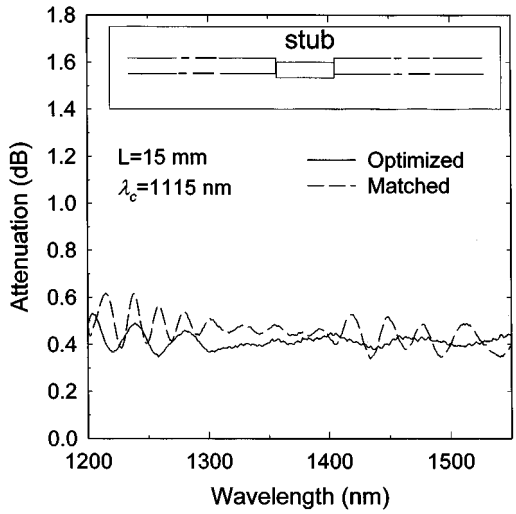

Fig. 10. Spectral attenuation of optimized and matched cladding fiber stubs in zirconia ferrule with 0.4 dB insertion loss.

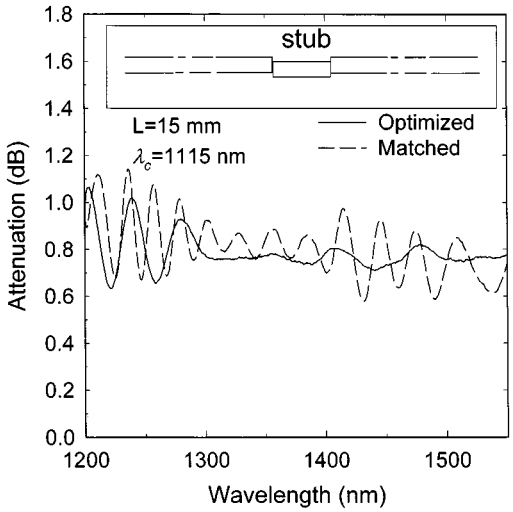

Fig. 11. Spectral attenuation of optimized and matched cladding fiber stubs in zirconia ferrule with 0.8 dB insertion loss.

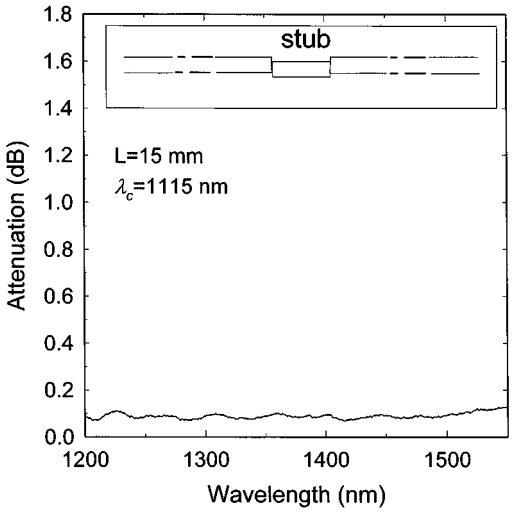

Fig. 12. Spectral attenuation of optimized fiber stub in zirconia ferrule with 0.1 dB insertion loss.

higher order modes. On the other hand, for the optimized fiber, the refractive index difference between the fiber and ferrule is less critical. For example, a refractive index change of 0.14 between the outer cladding and the ferrule will attenuate the higher order mode by 0.2 dB/cm for the case of the matched cladding fiber, and by 9 dB/cm for the case of the optimized fiber. The new fiber design makes the selection of the index matching material more flexible.

$$\eta_{jklm} = \frac{\int_{A'} \left|\Psi_{jk}(r,\theta)\Psi^*_{lm}(r',\theta')\,dA\right|^2}{\mathrm{Re}\left[\int_A \Psi_{jk}(r,\theta)\Psi^*_{jk}(r,\theta)\,dA\right]\mathrm{Re}\left[\int_A \Psi_{lm}(r,\theta)\Psi^*_{lm}(r,\theta)\,dA.\right]} \tag{6}$$

IV. Experimental Verification

The experimental setup for measuring the modal interference is shown schematically in Fig. 9. A 15-mm stub of single-mode fiber was connected to launching (A), and receiving (B), standard single-mode telecommunication fibers. Light from a tungsten-halogen lamp was passed through a monochromator and coupled into the launching fiber. The output light from the receiving fiber was measured with synchronous detection. A 3-cm loop was used in the launching and receiving fibers to ensure that the higher order modes are completely attenuated at the 1310 nm region.

To verify our theory, two fibers were made with similar cutoff wavelength: one corresponding to the optimized design in Fig. 7, and the other to a matched cladding fiber. The cutoff wavelength predicted from the equivalent step index model is 1124 nm for the optimized fiber, and 1115 nm for the matched cladding fiber.

Figs. 10 and 11 show the measured spectral attenuations of the two fibers inserted in zirconia ferrules with insertion losses of about 0.4 and 0.8 dB. As seen in these figures, the modal interference of the optimized fiber is significantly reduced. In the range of 1300–1550 nm, it is negligible for an insertion loss of 0.4 dB, and is only 0.1 dB for an insertion loss of 0.8 dB. Using the same optimized fiber, an insertion loss of less than 0.1 dB was achieved as shown in Fig. 12, indicating that the modal interference reduction does not result in additional loss penalty due to fiber mismatch.

V. Conclusion

We have presented a theoretical and experimental study on modal interference in field-mountable single-mode fiber connectors. The purpose of this work was to develop a fiber and connector ferrule assembly in which the modal interference is reduced significantly without increasing its insertion loss to a standard fiber. A theoretical model has been developed to analyze the modal interference. From this model, an optimized fiber design was derived. A series of modal interference measurements performed were in good agreement with the theory. Using an optimized fiber, a significant reduction in modal interference and very low insertion loss were achieved.

References

[1] M. De Jong, "Cleave and crimp fiber optic connector for field installation," in *Proc. OFC '90*, San Francisco, CA, paper ThA2.

[2] K. Abe, Y. Lacroix, L. Bonnell, and Z. Jakubczyk, "Modal interference in a short fiber section: Fiber length, splice loss, cutoff, and wavelength dependence," in *Proc. OFC '91*, San Diego, CA, 1991, paper ThA3.

[3] J. C. Goodwin and P. J. Vella, "Modal noise in short fiber sections," *J. Lightwave Technol.*, vol. 9, pp. 954–958, 1991.

[4] G. A. Olson and R. M. Fortenberry, "Modal noise in single-mode fiber-optic system with closely spaced splices," *Fiber Integr. Opt.*, vol. 9, pp. 237–245, 1990.

[5] D. A. Harris and R. A. Throckmorton, "Modal interference in field installable single-mode fiber-optic connectors," in *Proc. 1994 10th NFOEC*, vol. 3, 1994, pp. 399–406.

[6] D. A. Harris and R. A. Throckmorton, "Azimuthal dependence of modal interference in closely spaced single-mode fiber joints," *1994 Photon. Technol. Lett.*, vol. 6, pp. 1235–1237, 1994.

[7] D. A. Harris and R. A. Throckmorton, "Characterizing modal interference in field-installable single-mode fiber connectors incorporating short fiber stubs," in *1994 Tech. Dig. Symp.*, 1994, paper 864, pp. 35–38.

[8] D. G. Duff, F. T. Stone, and J. Wu, "Measurements of modal noise in single-mode lightwave system," in *Proc. OFC '85*, San Diego, CA, paper TUO1.

[9] S. Heckmann, "Modal noise in single-mode fibers operated slightly above cutoff," *Electron. Lett.*, vol. 17, pp. 499–450, 1981.

[10] A. W. Snyder and J. D. Love, *Optical Waveguide Theory*. London, U.K.: Chapman and Hall, 1983.

Ming-Jun Li, photograph and biography not available at the time of publication.

Costas Saravanos was born in Makrakomi, Greece, in 1951. He received the B.Sc. degree in physics from the University of Athens, Athens, Greece, the M.Sc. degree in electrical engineering from the South Dakota School of Mines, SD, and the Ph.D. degree in electrical engineering from the University of Ottawa, Ont., Canada.

From 1981 to 1994, he was with Nortel Optical Cable Division, initially as a Scientist and later as a Manager, in the development of single-mode fiber process, design, and characterization. Since 1994, he has been with Siecor, Keller, TX, where he is currently Manager of Advanced Technologies, working in the development of various areas of photonics.